Communication

Metal–Peroxo versus Metal–Oxo Oxidants in Non-Heme Iron-Catalyzed Olefin Oxidations: Computational and Experimental Studies on the Effect of Water

David Quionero, Keiji Morokuma, Djamaladdin G. Musaev, Rubn Mas-Ballest, and Lawrence Que

J. Am. Chem. Soc., **2005**, 127 (18), 6548-6549• DOI: 10.1021/ja051062y • Publication Date (Web): 15 April 2005

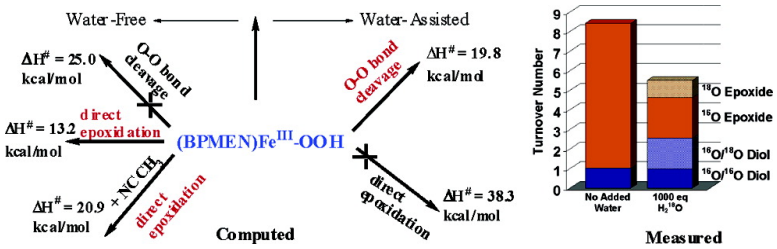

More About This Article

Additional resources and features associated with this article are available within the HTML version:

- Supporting Information
- Links to the 5 articles that cite this article, as of the time of this article download
- Access to high resolution figures
- Links to articles and content related to this article
- Copyright permission to reproduce figures and/or text from this article

View the Full Text HTML

J|A|C|S
COMMUNICATIONS

Published on Web 04/15/2005

Metal−Peroxo versus Metal−Oxo Oxidants in Non-Heme Iron-Catalyzed Olefin Oxidations: Computational and Experimental Studies on the Effect of Water

David Quiñonero, Keiji Morokuma,* and Djamaladdin G. Musaev*

Cherry L. Emerson Center for Scientific Computation and Department of Chemistry, Emory University, 1515 Dickey Drive, Atlanta, Georgia 30322

Rubén Mas-Ballesté and Lawrence Que Jr.*

Department of Chemistry and Center for Metals in Biocatalysis, University of Minnesota, Minneapolis, Minnesota 55455

Received February 18, 2005; E-mail: dmusaev@emory.edu; morokuma@emory.edu; que@chem.umn.edu

The emergence of a large family of mononuclear non-heme iron oxygenases has prompted the design and development of non-heme iron complexes that can catalyze alkane hydroxylation as well as olefin epoxidation and cis-dihydroxylation using H_2O_2 as an oxidant.[1] In many cases, high stereoselectivity is achieved. These bioinspired catalysts typically consist of a mononuclear iron(II) center coordinated to tetradentate N4 ligands, such as TPA [tris-(2-pyridylmethyl)amine] and BPMEN [*N*,*N*′-dimethyl-*N*,*N*′bis(2-pyridylmethyl)-1,2-diaminoethane].[1b−e] The more thoroughly studied TPA catalyst oxidizes cyclooctene to approximately equimolar amounts of epoxide and *cis*-diol and has been proposed to operate via an initial Fe^{III}−OOH intermediate that is converted to a *cis*-HO−Fe^{V}═O oxidant in a water-assisted mechanism. This hypothesis is best supported by the observation that one oxygen atom of the *cis*-diol product is derived from H_2O_2 and the other from added $H_2{}^{18}O$.[1c] Subsequent DFT calculations show that the unprecedented HO−Fe^{V}═O oxidant is energetically plausible.[2] Extending these notions to the BPMEN catalyst may require some adjustments to the mechanism since this catalyst oxidizes cyclooctene mainly to epoxide (*cis*-diol/epoxide ∼ 1:8).[1c] In line with ongoing literature discussion on heme-catalyzed oxidations regarding the viability of an iron(III)−peroxo oxidant versus the more commonly accepted high-valent oxoiron species,[3] we have compared by DFT calculations two alternative scenarios for olefin oxidation by Fe(BPMEN), one water-assisted (*wa*) and the other non-water-assisted (*nwa*) (Figure 1), which invoke the participation of either a *cis*-OH−Fe^{V}═O or an Fe^{III}−OOH oxidant. On the basis of these DFT results, we suggest that both pathways are energetically plausible and that the presence of water can alter the course of the olefin oxidation, and we have subsequently corroborated these conclusions by experiment.

Figure 1 summarizes our DFT results.[4] Let us first focus on (BPMEN)Fe^{III}−OOH, the common intermediate in the *wa* and *nwa* pathways. This intermediate may adopt two distinct structures, Fe^{III}−η^1−OOH (**1**) and Fe^{III}−η^2−OOH (**2**). Isomer **1** has a ^{6}A ground state with ^{4}A and ^{2}A spin states located 4.0 and 8.5 kcal/mol higher in energy, respectively, while isomer **2** exists only in ^{6}A and ^{2}A states (with the former slightly lower in energy than the latter). Optimization of **2** in the ^{4}A state converges to **1** without any energy barrier. The ground state of **1** is 6.7 kcal/mol lower in energy than that for **2**. Interconversion of the two isomers occurs with a very small energy barrier.

When water is absent (*nwa* mechanism), the reaction starts from either **1** or **2** and may proceed through two different pathways. One path involves initial cleavage of the O−OH bond followed by attack of the olefin, while the other proceeds by direct attack of

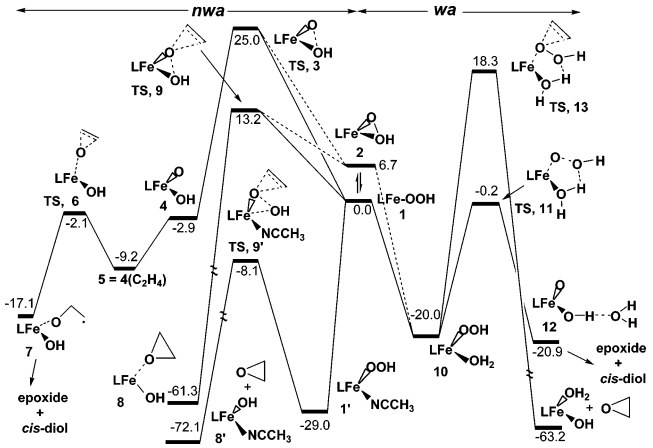

Figure 1. Schematic representation of the non-water-assisted (*nwa*) and water-assisted (*wa*) mechanisms of the (BPMEN)FeOOH-catalyzed epoxidation. Energies are given in kcal/mol and calculated relative to Fe^{III}−η^1−OOH + H_2O + $NCCH_3$ + C_2H_4 dissociation limit.

the olefin. The cleavage of the O−OH bond has an activation energy of 25.0 kcal/mol (below, we will discuss only the ground state energetics along the potential energy surfaces of the reactions studied) at the ^{2}A transition state (TS) **3**. This is in agreement with the experiments indicating that a low-spin Fe^{III} center activates the O−O bond more easily than its high-spin counterpart.[12] The product of the reaction is HO−Fe^{V}═O (**4**), which in its ^{4}A ground state, lies 2.9 kcal/mol lower than the reactant **1**. Epoxidation from **4** starts by formation of the **4**(C_2H_4) adduct, **5**, and occurs through multiple TSs and intermediates. The energy barrier at the first TS, **6**, is calculated to be 7.1 kcal/mol. Overcoming this barrier leads to intermediate **7**, which converts to the final epoxide and/or *cis*-diol products with an extremely small activation barrier. Since all barriers for epoxidation/cis-dihydroxylation starting from **4** are much smaller than the initial O−OH bond cleavage barrier of 25.0 kcal/mol, O−O bond cleavage is the rate-determining step.

An alternative route in the *nwa* pathway involves direct attack of Fe^{III}−OOH on olefin starting from **1** (or **2**). This step occurs via the concerted transition state **9** (with a ^{6}A ground state) and can only lead to olefin epoxidation. The activation barrier is 13.2 kcal/mol, which is 11.8 kcal/mol lower than that for the O−OH cleavage. Inclusion of the entropy effect reduces the Δ(TS-**9**−TS-**3**) from 11.8 to 6.2 kcal/mol. However, since the actual experiments are carried out in MeCN solvent, we also considered the effect of binding MeCN to (BPMEN)Fe^{III}(OOH) prior to its reaction with olefin. The calculations show that the coordination of MeCN increases the barrier for direct epoxidation by almost 8 kcal/mol,

10.1021/ja051062y CCC: $30.25

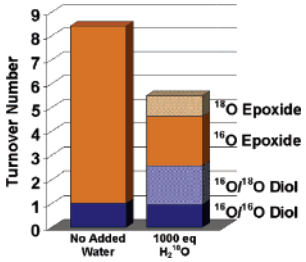

Figure 2. Yields (in moles diol or epoxide formed per mole catalyst) for the oxidation of cyclooctene by 10 equiv of H_2O_2 in the presence of [(BPMEN)Fe(OTf)$_2$] in CH_3CN (orange represents epoxide and blue *cis*-diol products).

but this barrier is still lower than that for O−O bond cleavage. Thus, in the absence of water, the calculations overwhelmingly favor the direct attack pathway for the Fe(BPMEN)OOH oxidant leading exclusively to epoxidation.

Next, we consider the *wa* mechanism, centered on the six-coordinate (BPMEN)(H_2O)Fe^{III}(OOH) **10** with a ^{2}A ground state. From this species, the reaction may proceed again via two different pathways. The pathway starting with the O−OH bond cleavage occurs with a 19.8 kcal/mol barrier (relative to complex **10**) at the ^{2}A TS **11**. From the resulting intermediate **12**, the process has to follow a mechanism very similar to that of *nwa* **4** and leads to both epoxide and *cis*-diol products. As expected, complex **12** and its TPA analogue (TPA-**12**) reported previously[2] have many similarities. Indeed, the ground state for both compounds is ^{4}A with similar Fe=O (1.672 and 1.665 Å for **12** and TPA-**12**, respectively) and Fe−OH (1.757 and 1.765 Å for **12** and TPA-**12**, respectively) bond lengths. Moreover, they both have almost identical spin densities on the Fe and O atoms. The barrier for O−OH bond cleavage is almost one-half of the 38.3 kcal/mol barrier for direct epoxidation by the same complex **10** at the ^{2}A transition state **13**. Therefore, one may expect that, when water is present, olefin oxidation by Fe(BPMEN) occurs via the HO−Fe^V=O species **12**, as opposed to the Fe^{III}−OOH species when water is not present. Furthermore, the *wa* pathway proceeds via the low-spin state, while in the *nwa* pathway, the high-spin process is kinetically and thermodynamically more favorable.

We have sought to test the DFT-derived notions with experiments, and the results obtained are fully consistent with these theoretical findings (Figure 2). As previously reported, Fe(BPMEN)-catalyzed cyclooctene oxidation under our typical conditions yields 8.4 turnovers of product (from 10 equiv of H_2O_2) with a diol/epoxide ratio of 0.13. In the presence of 1000 equiv of added water, the number of turnovers decreases to 5.5, but the diol/epoxide ratio increases almost 7-fold, due to the diol more than doubling in yield and epoxide decreasing by more than a factor of 2. The much larger diol/epoxide ratio in the presence of water suggests that the *wa* mechanism has become more dominant under these conditions.

^{18}O-labeling experiments support this conclusion. In the presence of 1000 equiv of $H_2{}^{18}O$, the epoxide product shows 30% incorporation of labeled oxygen. Considering that sole operation of the *wa* mechanisms should give 50% labeled epoxide due to facile oxo/hydroxo tautomerization of the putative 2-fold-symmetric HO−Fe^V=O oxidant **12**, this result indicates that, in the presence of 1000 equiv of water, 60% of the epoxide obtained must come from the *wa* pathway, and the remaining 40% should arise from the *nwa* mechanism. A similar 60:40 partitioning can also be deduced for diol formation, as 60% of the diol product shows incorporation of one labeled oxygen, as expected for the *wa* pathway. Thus by inference, the *nwa* mechanism must be dominant under conditions with much less water.

In summary, our computational and experimental studies show that Fe(BPMEN)-catalyzed olefin oxidation has a complex reaction mechanism that allows both Fe^{III}−OOH and Fe^V=O species to act as oxidants with comparable activation barriers. The presence of water favors formation of an HO−Fe^V=O oxidant via water-assisted O−OH bond cleavage and leads to both epoxide and *cis*-diol products. In its absence, the oxidant is the Fe^{III}−OOH (or (MeCN)-Fe^{III}−OOH), and oxidation mainly leads to epoxide. This conclusion differs from that derived from DFT investigations of iron−porphyrin-catalyzed olefin epoxidation, where the Fe^{III}−OOH pathway is deemed too high in energy to be plausible.[3c,13] The difference between these two systems may lie in the more flexible coordination environment of the non-heme iron complex, which has an available adjacent coordination site that contributes to the activation of the peroxide in both *wa* and *nwa* pathways.

Acknowledgment. D.Q. and R.M. thank the Ministerio de Educación y Ciencia of Spain for postdoctoral support. The present research is supported by grants from NSF (CHE-0209660 to K.M. and D.G.M.) and DOE (FG02-03ER15455 to L.Q.).

Supporting Information Available: Experimental procedure, complete ref 11, and Cartesian coordinates of all discussed structures. This material is available free of charge via the Internet at http://pubs.acs.org.

References

(1) (a) Costas, M.; Mehn, M. P.; Jensen, M. P.; Que, L., Jr. *Chem. Rev.* **2004**, *104*, 939. (b) Chen, K.; Costas, M.; Que, L., Jr. *Dalton Trans.* **2002**, 672. (c) Chen, K.; Costas, M.; Kim, J.; Tipton, A. K.; Que, L., Jr. *J. Am. Chem. Soc.* **2002**, *124*, 3026. (d) Costas, M.; Que, L., Jr. *Angew. Chem., Int. Ed.* **2002**, *41*, 2179. (e) Fujita, M.; Costas, M.; Que, L., Jr. *J. Am. Chem. Soc.* **2003**, *125*, 9912.

(2) Bassan, A.; Blomberg, M. R. A.; Siegbahn, P. E. M.; Que, L., Jr. *J. Am. Chem. Soc.* **2002**, *124*, 11056.

(3) (a) Jin, S.; Bryson, T. A.; Dawson, J. H. *J. Biol. Inorg. Chem.* **2004**, *9*, 644. (b) Nam, W.; Ryu, Y. O.; Song, W. J. *J. Biol. Inorg. Chem.* **2004**, *9*, 654. (c) Shaik, S.; de Visser, S. O.; Kumar, D. *J. Biol. Inorg. Chem.* **2004**, *9*, 661. (d) Que, L., Jr. *J. Biol. Inorg. Chem.* **2004**, *9*, 684.

(4) Computational Methods. The geometry of the reported compounds was optimized at the B3LYP level[5] in junction of the LANL2DZ basis set with associated ECP for Fe.[8] The energies[9] were further refined by single point calculations at the B3LYP/LANL2DZ geometries using the SDD basis set with associated ECP for Fe[10] and 6-311+G(d) basis sets on the other atoms as implemented in the Gaussian 03 program.[11]

(5) Previously, we have demonstrated[6] that the hybrid B3LYP method describes the low-lying electronic states of the [(BPMEN)Fe^{II}(NCCH$_3$)$_2$]$^{2+}$ precursor complex better than the nonhybrid BP86 method. Despite this fact, we still believe that the B3LYP method used in this paper slightly overestimates the high-spin states, as demonstrated earlier,[7] and the obtained small energy gap between the high-spin and low-spin states of the Fe−OOH complexes needs to be taken with caution.

(6) Quiñonero, D.; Musaev, D. G.; Morokuma, K. *Inorg. Chem.* **2003**, *42*, 8449.

(7) (a) Lynch, B. J.; Fast, P. L.; Harris, M.; Truhlar, D. G. *J. Phys. Chem. A* **2000**, *104*, 4811. (b) Musaev, D. G.; Geletii, Y. A.; Hill, G.; Hirao, K. *J. Am. Chem. Soc.* **2003**, *125*, 3877.

(8) Hay, P. J.; Wadt, W. R. *J. Chem. Phys.* **1985**, *82*, 270.

(9) Energies given in this paper are enthalpies (at T = 298.15 K and pressure = 1 atm).

(10) Dolg, M.; Wedig, U.; Stoll, H.; Preuss, H. *J. Chem. Phys.* **1987**, *86*, 866.

(11) Frisch, M. J. et al. *Gaussian 03*, revision B.01; Gaussian, Inc.: Pittsburgh, PA, 2003.

(12) (a) Ho, R. Y. N.; Roelfes, G.; Feringa, B. L.; Que, L., Jr. *J. Am. Chem. Soc.* **1999**, *121*, 264. (b) Lehnert, N.; Ho, R. Y. N.; Que, L., Jr.; Solomon, E. I. *J. Am. Chem. Soc.* **2001**, *123*, 8271.

(13) (a) Ogliaro, F.; de Visser, S. P.; Cohen, S.; Sharma, P. K.; Shaik, S. *J. Am. Chem. Soc.* **2002**, *124*, 2806. (b) Kamachi, T.; Shiota, Y.; Yoshizawa, K. *Bull. Chem. Soc. Jpn.* **2003**, *76*, 721.

JA051062Y